The Patlak Plot in MRI Pharmacokinetic Analysis

C. S. Springer, Jr. [1], W. D. Rooney[1], and X. Li[1]
[1]Advanced Imaging Research Center, Oregon Health & Science University, Portland, Oregon, United States

Introduction: An honored method for pharmacokinetic interpretation is the Patlak Plot (PP) – the popular linearization technique introduced over 25 years ago (1) for graphical tracer data analyses. The PP is reviewed [and used for rat glioma model MRI data] in (2). In (Dynamic-Contrast-Enhanced) DCE-MRI, the injected contrast reagent (CR) plays the tracer role. The integral pharmacokinetic rate law upon which the PP is generally based is given in Eq. [1]: where v_e is the extracellular

$$v_e[CR_o](T) + v_p[CR_p](T) = K^{trans}\int_0^T [CR_p](t)e^{(-K^{trans}v_e^{-1}(T-t))}dt + v_p[CR_p](T) \qquad [1]$$

extravascular volume fraction, $[CR_o]$ is the interstitial CR concentration, v_p and $[CR_p]$ are the blood plasma volume fraction and CR concentration, respectively, and K^{trans} measures the CR extravasation rate [a volume fraction unidirectional rate constant product (3)]. The Eq. [1] LHS is the tissue CR concentration, $[CR_t]$, the amount of CR per voxel volume. This is what is measured with a tracer, for which the signal is not compartment-specific. Taking a radiotracer as an example, its voxel signal (*e.g.*, disintegrations per second) is directly proportional to $[CR_t]$. [Careful work accounts for the simultaneous, and independent, tracer activity decay.] The Patlak Plot has $\{[v_e[CR_o](T) + v_p[CR_p](T)]/[CR_p](T)\}$ as ordinate and $\{[\int_0^T [CR_p](t)e^{(-K^{trans}v_e^{-1}(T-t))}dt\,]/[CR_p](T)\}$ as abscissa: the integration limit T is incremented. Thus, with $[CR_p](T)$ [the arterial input function (AIF)] measured, implementing Eq. [1] is straightforward for tracers.

However, a crucial tracer/CR difference enters prior to Eq. [1] in the model derivation (4). Since MR images are made from the water proton MR signal (^1H_2O), the signal molecule (water) is not the same as the tracer molecule (CR). These are never distributed equally in tissue. Though intercompartmental water transfer is generally faster than CR transfer, it is not infinitely so. Major consequences of this are that MRI signal properties are usually not linearly proportional to [CR], and that, for DCE-MRI (which employs T_1-weighted ^1H_2O signals), the sub-voxel compartmental signals are intrinsically discriminated during the DCE-MRI acquisition time-course (3,4). It is well-known that the MR steady-state signal strength (S) is not linearly proportional to the ^1H_2O longitudinal relaxation rate constant (R_1) value $[R_1 \equiv (T_1)^{-1}]$ (3). It is also true that, except for blood, R_1 is not linearly proportional to most tissue [CR]: the coefficient between these (the "effective" relaxivity, r_1) decreases continually as [CR] increases (3). This is true because equilibrium intercompartmental water exchange kinetics are finite (3). This means it is not correct to substitute voxel R_1 (or, worse, S) values linearly for [CR] values in order to use Eq. [1] for graphical analysis.

However, such an approach is usually tried. The second generation Standard Model (SM2) for DCE-MRI assumes that $[v_e[CR_o](T) + v_p[CR_p](T)]$ bears a linear relationship to the tissue ^1H_2O $R_1(T)$ that is measured, *via* the r_1 coefficient, and that $(1 - h_v)v_p[CR_p](T)$ is linearly related to the blood ^1H_2O $R_{1b}(T)$ [h_v is the macrovessel blood hematocrit]. Though (as above) the latter is almost always a good approximation, the first assumption implies that both the equilibrium transendothelial and transcytolemmal water exchange kinetics are effectively infinitely fast (3,4). The MR exchange systems for these two processes are constrained to each remain in their Fast-eXchange-Limit [FXL] conditions throughout the DCE-MRI acquisition. Furthermore, the simple addition of the "indicator dilution" $v_p[CR_p]$ term on the Eq. [1] RHS also implies that the transendothelial exchange system remains in its FXL condition (5). We show the consequences of these assumptions.

Methods: We employ 12T DCE-MRI data from a cerebrally-implanted rat brain U87 glioma ROI that have been reported elsewhere (6). Experimental details [including the AIF, $[CR_p](T)$] are provided there. The DCE-MRI signal intensity time-course data are well-fitted with the second generation Shutter-Speed Model (SSM2) (4) using a successive approach (6), and this yields $[CR_o](T)$.

Results: Setting the SSM2 mean vascular and intracellular water lifetime (τ_b and τ_i, respectively) values each to 1 ms (vanishingly small) approximates the SM2. Fitting the data with these assumptions leads to the Patlak Plot with filled squares in the inset of the **Figure** panel a. It is linear with slope $K^{trans} = 0.31$ min^{-1} and intercept $v_p = 0.021$ ($v_b = [v_p/(1 - h_s)] = 0.030$: v_b is the blood volume fraction; $h_s = 0.3$, the microvessel hematocrit.) The *initial portion* is zoomed in the main panel a.

Setting τ_b and τ_i each to finite values admits the possibility of exchange effects: *i.e.*, allows that [CR] values can potentially transiently determine voxel ^1H_2O R_1 values nonlinearly during the bolus time-course. Panel a also shows the PP that results when the same data were analyzed with SSM2 and τ_b and τ_i each fixed at 300 ms [a reasonable value (7)] (filled circles). Though the plot is just as linear and has the same slope, it has a different intercept: $v_p = 0.025$ ($v_b = 0.036$). Each entire PP is an excellent straight line (both are in panel a inset). The shift of this line is a demonstration of a shutter-speed (water exchange) effect. The Standard Model v_b is 17% lower than the Shutter-Speed Model v_b, and this is clearly outside of experimental error (panel a).

Panel b shows the PP when CR re-intravasation, described by the exponential factor within the Eq. [1] RHS integrand is ignored [by assuming K^{trans}/v_e is zero] (open circles). The nonlinearity clearly indicates that there is significant blood CR reentry in this tumor, and its neglect becomes noticeable quite quickly.

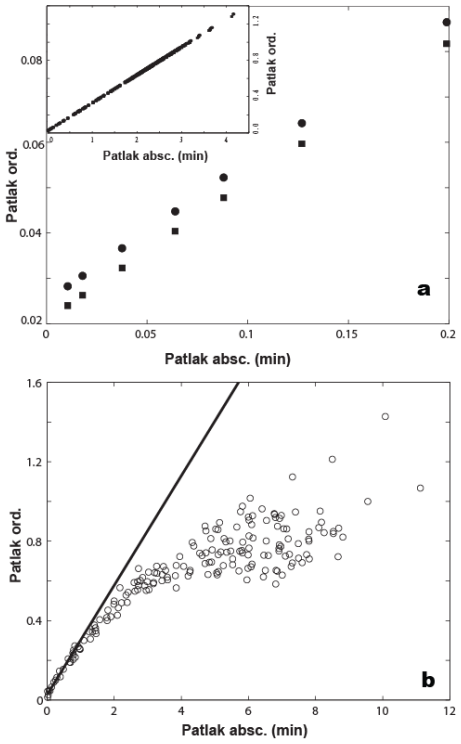

Discussion: It is clear that using SM2 to relegate CR to tracer status, and obtaining a linear Patlak Plot, does not in itself validate the assumptions required to do so. This case reported here is one where there is no significant shutter-speed effect on K^{trans}, but there is on v_b. Since model DCE-MRI data fitting must be accomplished beforehand (and this yields pharmacokinetic parameters), the Patlak Plot seems somewhat redundant. With sufficient signal-to-noise and exchange-sensitivity (3), SSM2 can also allow estimation of τ_b and/or τ_i, and thus endothelial and/or cytolemmal P_WS $[(v_b/\tau_b)$ and/or (v_e/τ_i), respectively (3)] – the water permeability coefficient surface area products. Since $K^{trans} \approx K_{CR}S$ for endothelium (5), $P_WS/P_{CR}S = P_W/P_{CR}$ for endothelium.

Grant Support: NIH: RO1-NS40801, RO1-EB00422, RO1-EB007258, NMSS RG 3168-A-1.

References: 1. Patlak, Blasberg, Fenstermacher, *JCBFM* **3**:1-7 (1983). **2.** Ewing, Brown, Lu, Panda, Ding, Knight, Cao, Jiang, Nagaraja, Churchman, Fenstermacher, *JCBFM* **26**:310-320 (2006). **3.** Li, Huang, Morris, Tudorica, Seshan, Rooney, Tagge, Wang, Xu, Springer, *PNAS* **105**:17937-17942 (2008). **4.** Li, Rooney, Springer, *MRM* **54**:1351-1359 (2005) [Erratum; *MRM* **55**:1217 (2006)]. **5.** Li, Springer, Jerosch-Herold, *NMR Biomed* **22**:148-157 (2009). **6.** Li, Rooney, Varallyay, Goodman, Selzer, Tagge, Pike, Neuwelt, Springer, *PISMRM* **16**:3827 (2008). **7.** Donahue, Weisskoff, Chesler, Kwong, Bogdanov, Mandeville, Rosen, *MRM* **36**:858-867 (1996).